The Nonuniform Distribution of Inclusions in Low-Alloy Steel Weld Deposits

A. A. B. SUGDEN and H. K. D. H. BHADESHIA

Nonmetallic inclusions in low-alloy steel welds have an important effect on the microstructure and properties of weld deposits. This work is an attempt at understanding the factors controlling the spatial distribution of such inclusions, with particular emphasis on the uniformity of the distribution and the effect of solidification mode during manual-metal-arc welding. The solidification mode has been controlled by using unusual combinations of base plates and experimental electrodes. It is found that the first phase to solidify (in the form of columnar grains) is delta-ferrite (δ) when a medium carbon electrode is deposited onto a low carbon substrate, but that it is austenite (γ) when a low carbon electrode is deposited onto a high carbon substrate. Relatively large inclusions have been found to position themselves preferentially, during solidification, to the columnar grain boundaries of the first phase to solidify, whether this is δ-ferrite or austenite. The results can be understood qualitatively in terms of a surface tension driven Marangoni effect, or in terms of the pushing of solid inclusions by the solidification front. Both mechanisms drive the larger inclusions into cusps in the interface while smaller ones are passively trapped. The implications of the observed nonuniform distribution of inclusions are more severe for solidification with austenite as the primary phase, since the larger inclusions are in that case located in the weakest region of the weld where they also do not contribute to the intragranular nucleation of acicular ferrite.

I. INTRODUCTION

IN order to satisfy the ever increasing demand for improvements in the toughness of weld deposits in engineering structures, there is strong incentive to improve welding consumables and to design new welding methods.[1] To do this systematically requires a method for modeling the microstructure and properties of welds as a function of its chemical composition, thermal history, and many other variables.

The microstructure of a steel weld is complex; solidification involves the epitaxial growth of δ-ferrite from the parent plate grains at the fusion boundary, and because of the high temperature gradients involved in arc welding it proceeds in a cellular manner. The resulting solid δ-ferrite grains have an anisotropic columnar morphology. On further cooling, austenite forms in such a way that its final grain structure resembles closely the original δ-ferrite morphology. However, if the carbon level or the substitutional alloy content or cooling rate is sufficiently high, then austenite is the first solid to form and columnar austenite grains grow directly from the melt. This is because of the small differences in the free energies of the two phases.[2] Whatever the mechanism of primary solidification, the austenite grains eventually undergo further transformation into a complex microstructure (described elsewhere[3]) consisting of layers of allotriomorphic ferrite which decorate the austenite grain boundaries, Widmanstätten ferrite plates, intragranularly nucleated acicular ferrite plates, and small amounts of martensite or degenerate pearlite. This is the "as-welded" microstructure, and it can have a profound influence on mechanical properties. For example, the layers of allotriomorphic ferrite are understood to be detrimental

to toughness,[4,5,6] whereas the morphology of acicular ferrite ensures that any crack has to follow a tortuous path during propagation, thus imparting better toughness to the weld.[6,7,8]

A model now exists which is capable of estimating quantitatively the microstructure of the fusion zone of low-alloy steel welds, as a function of their chemical composition and welding conditions.[3] The model does not, however, reveal any information about nonmetallic inclusions which are inevitably present in welds. Inclusions in welds originate from oxides formed during weld deposition, or from the unintentional trapping of slag forming materials which are used to protect the molten metal during welding. Inclusions are known to initiate fracture in weld metals,[9–12] so their content should be kept to a minimum. On the other hand, it is also believed that they are responsible for the intragranular nucleation of acicular ferrite,[13,14,15] a highly desirable phase from the point of view of toughness. In order to reach a compromise inclusion content with the right size distribution, it is essential that a method is developed for quantitatively predicting the important characteristics of inclusions in welds.

The present work is part of a program on the prediction of the microstructure and properties of weld deposits. For reasons which will become clear later, it attempts specifically to establish whether inclusions in low-alloy steel weld deposits are distributed uniformly throughout the weld. It has generally been assumed that the inclusions are randomly distributed. A variety of evidence suggests that this may not be the case. Uhlmann et al.,[16] Cissé and Bolling,[17,18] and others[19] have shown (using organic and other solid-liquid-particle systems) that a moving interface can push some particles ahead of it while others are trapped passively by the advancing interface. For cellular solidification, the pushed particles can then locate themselves into crevices in the interface (e.g., cell boundaries) where they are subsequently enclosed by the solid, leading to a nonuniform distribution of inclusions, with larger particles decorating the cell boundaries.

A. A. B. SUGDEN, Research Student, and H. K. D. H. BHADESHIA, University Lecturer, are with the Department of Materials Science and Metallurgy, University of Cambridge, Pembroke Street, Cambridge CB2 3QZ, United Kingdom.

Since the distribution of inclusions in the weld microstructure is determined during solidification when the inclusions are mobile in the melt, it seems possible that similar behavior should occur during weld-metal solidification, which might provoke a nonuniform distribution of inclusions, perhaps to the columnar grain boundary sites where they would do the most damage.

For a steel solidifying as δ-ferrite, the preferential location of the inclusions at the columnar boundaries would be advantageous since the subsequent austenite transformation would cause the inclusions to finish up in or near the center of the columnar austenite grain boundaries (Figure 1(a)). This is because the austenite grain boundaries would not coincide with the δ grain boundaries. Any inclusions at δ boundaries would not then be at the austenite boundaries.

The nucleation rate of acicular ferrite might be enhanced by the increased number of inclusions present in regions away from the austenite grain boundaries.

On the other hand, if solidification occurs with austenite as the primary phase, then there would be a nonuniform distribution of relatively large inclusions at the austenite grain boundaries (Figure 1(b)). In such circumstances, not only may the amount of acicular ferrite obtained in the final microstructure be reduced, but there would also be a concentration of inclusions in the weakest phase, allotriomorphic ferrite, which forms at the austenite grain boundaries. If inclusions enhance the grain boundary nucleation rate of allotriomorphic ferrite, then the situation would worsen since the volume fraction of undesirable allotriomorphic ferrite in the final microstructure would increase.
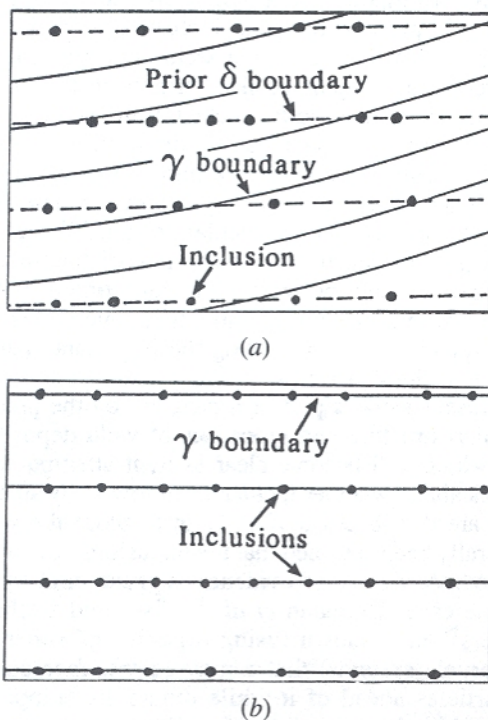

(a)

(b)

Fig. 1 — Schematic diagram showing the location of inclusions in the microstructure of a weld for solidification as (a) δ-ferrite and (b) austenite, assuming that the inclusions locate themselves preferentially at the cell boundaries during solidification. In (a) the prior δ-ferrite boundaries and austenite boundaries diverge, since in arc welding the heat source is not stationary.[20]

The aim of this particular work was to establish whether any preferential distribution of inclusions occurs during weld metal solidification, as a function of the solidification mode.

II. EXPERIMENTAL METHOD

To test for inclusion redistribution during solidification, two low-alloy steel manual-metal-arc welds were fabricated.

For one of the welds (Weld 1) a low carbon electrode was welded onto an 11 mm thick, Fe-0.68C-1.02Mn-0.24Si-0.03P-0.03S wt pct high carbon base plate using the bead-on-plate technique. According to the Fe-C equilibrium phase diagram, the high carbon concentration in the base plate will ensure that it is in the austenitic state before melting. In fact, solidification during welding is nonequilibrious, but this can only stimulate further the tendency to form austenite rather than δ-ferrite. Furthermore, since grain growth at the fusion boundary is epitaxial, this would ensure austenitic solidification of the entire weld pool even though the deposit itself has a relatively low-carbon concentration. This is because there is far less nucleation occurring within the weld pool itself.

In order to study a weld which solidifies initially as δ-ferrite, a second weld (Weld 2) was deposited using an experimental medium carbon electrode. The electrode was clad onto a Fe-0.12C-0.55Mn wt pct base plate. Six runs, in a layer sequence 3-2-1 were used, so that dilution of the top bead, which was the bead examined, would be minimal. This procedure gave a medium carbon weld which solidified as δ-ferrite.

In both cases, direct current (electrode positive) was employed, using a high current-low voltage (180 A/23 V) electric arc. The welding speed was approximately 4 mm · s^{-1}. Weld metal analyses are given in Table I.

The welds were sectioned, ground, and polished in oil prior to etching in order to avoid specimen pitting. The scanning electron micrograph (Figure 5) was taken using a Cambridge Stereoscan scanning electron microscope.

III. RESULTS

A. Weld 1: Primary Austenite Solidification

In Weld 1 the first phase to solidify was found to be austenite. This was indicated by the large amount of pearlite within the grains and the epitaxial growth at the fusion boundary, from a high carbon base plate whose structure at its melting point is austenite (Figure 2).

The microstructure of the weld metal showed irregular grains of acicular ferrite (α_a) and pearlite (dark etch), bounded by thin layers of allotriomorphic ferrite (α). Close to the fusion boundary, a substantial amount of Widmanstätten ferrite (α_w) was also evident. The heat-affected base metal contained a large amount of retained austenite, (γ_r).

Table I. Weld Metal Analyses

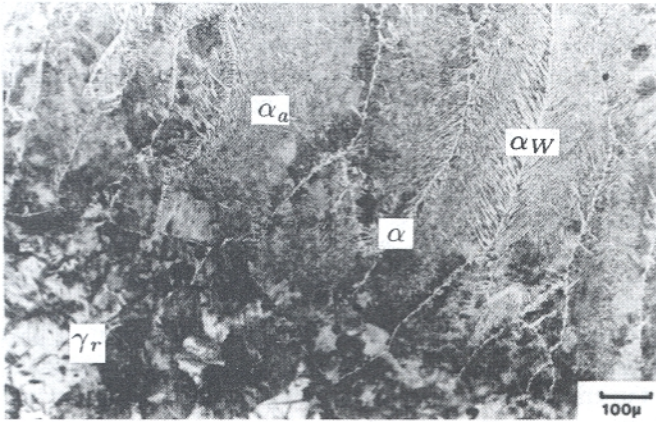| Weld	Solidification Mode	Composition/Wt Pct				
		C	Mn	Si	P	S
1	austenitic	0.29	0.76	0.20	0.16	0.15
2	ferritic	0.19	1.40	0.69	0.012	0.07

Fig. 2 — Weld 1: Microstructure at the fusion boundary for a weld solidifying as primary austenite. Note the curvature of the columnar grains due to the transient nature of the heat flow in the solidifying weld.

It is known that during solidification the weld metal comprises a series of columnar grains growing inward from the fusion boundary, each grain consisting of a bundle of fine regular hexagonal cells all having approximately the same crystallographic orientation in space.[21] This behavior leads to regions of microphases aligned along the cell boundaries, indicating a local difference in chemical composition within the columnar grains, and Figure 3 shows this segregation pattern. The cells within the grains change orientation only at the columnar boundaries, confirming that the weld solidified as austenite.
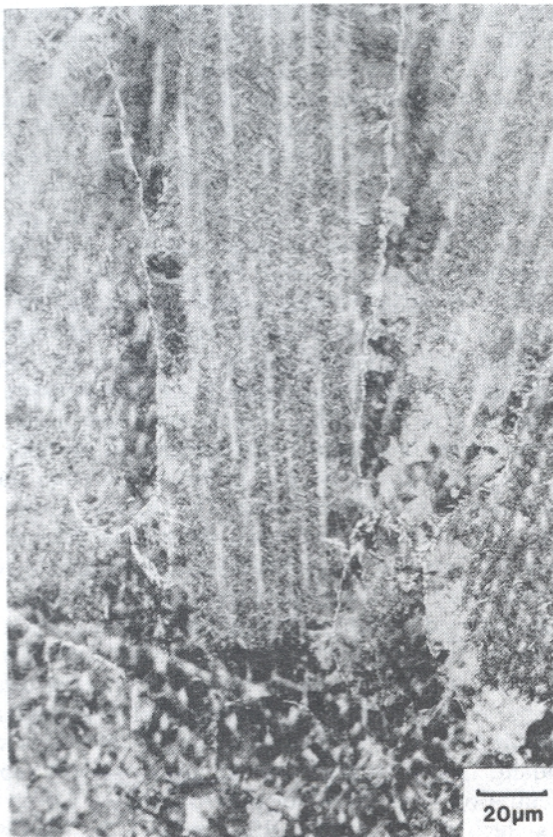
On etching Weld 1 with picral, large inclusions were observed at the columnar grain boundaries (Figure 4).

Figure 5 is a scanning electron micrograph of the same weld etched in bromine in methanol, which attacks the metal, but not inclusions.[22] It can be seen that there is a predominance of inclusions at the prior austenite grain boundaries. Note that this technique is used simply to confirm the presence of inclusions at the boundaries, and is not generally applicable since some inclusions may be washed away.

B. Weld 2: Primary Ferrite Solidification

The microstructure of Weld 2 (Figure 6) was typical of that of a low-carbon manganese steel weldment, and showed a columnar structure with layers of allotriomorphic ferrite at the prior austenite grain boundaries and fine plates of acicular ferrite within the grains. Clusters of Widmanstätten ferrite plates can be seen at the prior austenite grain boundaries.

Weld 2 solidified as δ-ferrite and subsequently transformed to columnar austenite grains. The nature of the original δ-ferrite solidification structure was not obvious, because the transformation to austenite during cooling destroys any microstructural evidence of the position of the
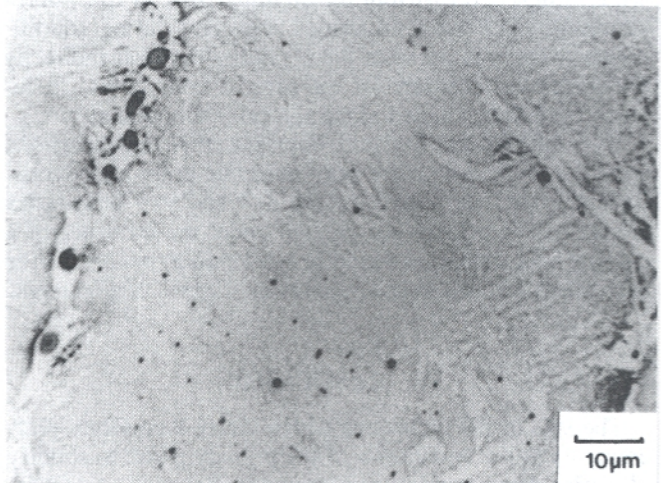

Fig. 4 — Weld 1: Large inclusions are located predominantly at the grain boundaries of the solidifying phase (austenite).
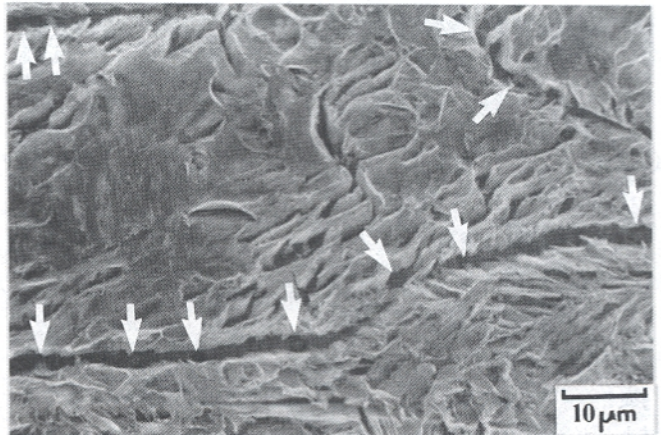

Fig. 3 — Weld 1: Epitaxial growth at the fusion boundary. The austenite solidification structure may be seen within the columnar grains.

Fig. 5 — Weld 1: Secondary electron image of deep-etched weld metal, showing inclusions (arrowed) at the columnar grain boundaries.
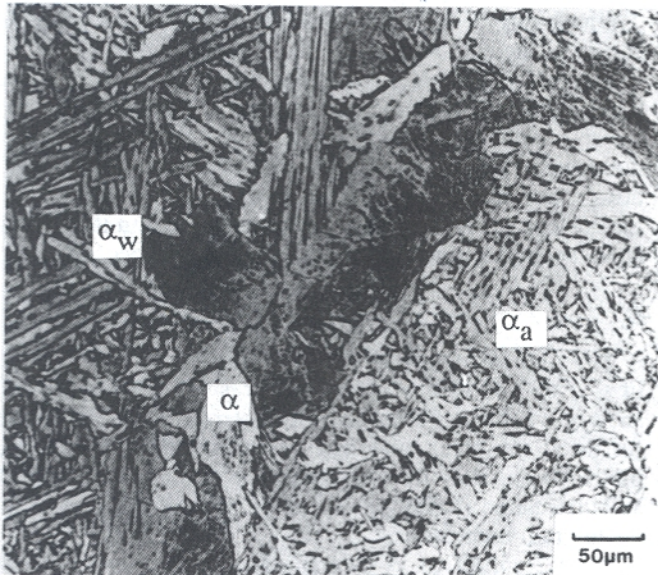
Fig. 6—Weld 2: Weld metal microstructure.

δ-δ grain boundaries. It could, however, be revealed by solute sensitive etching using Klemm I reagent (Figure 7), which maps the distribution of impurities in the microstructure; since these impurities segregate during solidification to regions between the δ grains, the etch indirectly delineates the positions of the prior δ boundaries. Inclusions were seen aligned along the prior δ-boundaries.

It should be emphasized, however, that the inclusions were not aligned with the prior austenite grain boundaries. Recent work[20] indicates that the δ/δ and γ/γ boundaries are neither coincident nor parallel under the influence of a moving heat source, as found in arc welding, but cross over each other, and this would account for the lack of alignment.

IV. DISCUSSION

The size of the inclusions which locate themselves preferentially at the boundaries of the primary phase to solidify identifies them as primary indigenous inclusions—that is, the deoxidation products of nonexternal origin which are present in the liquid during the freezing of the weld. They
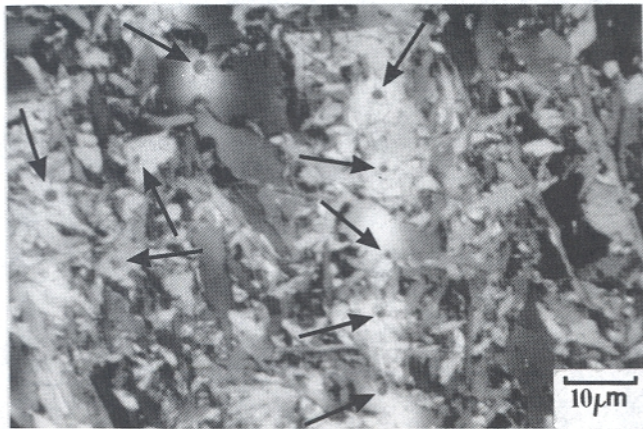

Fig. 7—Weld 2: Inclusions (arrowed) delineate the prior δ grain boundaries.

typically have dimensions ranging from 1 to 3 μm for arc welding of the type considered here.[23]

The nucleation, growth, and flotation of deoxidation products in liquid steel has been modeled by Turkdogan,[24] when the rate of nucleation in a weld is estimated by equating the number of nuclei to the number of inclusions found empirically. Knowing this, and the rate of growth of the inclusions, which is assumed to be limited by the diffusion of reactants to the surface of the inclusions, the rate of oxygen removal from the melt can be calculated. We find that for a weld metal, with a typical inclusion density of 10^7 mm^{-3}, the inclusions should grow to almost their ultimate size in less than one second, implying that flotation is the critical process in determining the final inclusion and oxygen content of a weld.

Stokes' law states that the velocity of an ascending spherical inclusion is

$$v = 2gr^2 \frac{(\rho_s - \rho_i)}{9\eta} \qquad [1]$$

where r is the radius of the sphere,
   ρ_s is the density of the steel,
   ρ_i is the density of the inclusion, and
   η is the coefficient of viscosity for the steel.

However, according to Stokes' law, if the weld pool is molten for, say, 5 seconds, the greatest distance traveled by, for example, a 1 μm inclusion will be only 1.7 μm. Thus, Stokes' law cannot be a critical factor in the removal of small inclusions of the type considered here, although the suggestion that it does not control the deoxidation of welds is less certain for larger particles. As far as the present work is concerned, Stokes' law implies that the upward flow of small inclusions during solidification can be neglected. These conclusions concur with those of Grong et al.,[25] who studied the silicon-manganese deoxidation of mild and low-alloy steel weld metals. Weld pool conditions are extremely turbulent with temperatures beneath the arc exceeding perhaps 3000 °C. This is especially true of arc welding, when electromagnetic stirring of the weld pool generated by Lorentz forces creates conditions of considerable turbulence within the pool.[26] However, this turbulence ceases as the heat source recedes and the temperature in the melt is reduced.[27] Grong et al. modeled deoxidation as a two-stage process. Above about 1900 °C continuous phase separation takes place as a consequence of turbulent flow conditions. In the cooler part of the weld pool, however, precipitated slag remains in the metal as finely dispersed particles. The solidification front during manual-metal-arc welding moves typically at a speed of 2 mm · s^{-1},[28] whereas the small inclusions float at just 0.5 μm · s^{-1} so that the solidification front grows into a melt containing virtually stationary small particles.

The observed preferential location of inclusions at the boundaries between grains of the primary phase can be understood as follows. Inclusions in welds, being usually based on mixed (MnAl) silicates and oxides, are assumed to exhibit fully incoherent (high energy) interfaces with the liquid. Interfacial tension is highly sensitive to solute concentration, and the adsorption of surface active elements, such as oxygen or sulfur, reduces the interfacial tension in slag-metal systems. Thus, a gradient of concentration of surface active elements along an interface can

result in a gradient of interfacial tension, and a concomitant interfacial flow. Such interfacial convection is usually called the "Marangoni effect".[29] This phenomenon, or some other force, perhaps surface tension, could explain the observed nonuniform distribution. Surface tension would tend to pull inclusions into the line of intersection among three grains. The solute-rich cell boundaries solidify at a lower temperature than the leading interface, and shrinkage during solidification, as well as the general motion of the interface, would tend to draw the inclusions in. The final structure would therefore contain more, and relatively larger particles, at the grain boundaries of the primary phase.

It should be noted that there are other possible mechanisms by which inclusions may end up preferentially at cusps in the solid-liquid interface, particularly if the interface can "push" inclusions in its direction of motion. Such an effect has been observed previously; Cissé and Bolling[18] and Uhlmann et al.[16] explained the observed pushing of particles by a solid-liquid interface in terms of a short range repulsive force between the particle and solid. However, work carried out by Weinberg,[30] in which the interaction of iron particles with a dendritic interface in a microgravity environment was studied, indicates that particles in a metal melt are not repelled by an advancing solid-liquid interface. Similarly, Schvezov and Weinberg carried out a series of modeling experiments, but found no evidence of particle interface repulsion.[31] They considered that the Lifshitz-Van der Waals force might cause repulsion of a metal particle in a liquid metal, but, in fact, found it to be positive.

In another experiment, using nylon spheres for particles, and a lucite cellular surface as an interface, Schvezov and Weinberg found that the spheres pushed by the interface tended to locate themselves preferentially at the cell boundaries as the interface advanced, rather than be trapped in the matrix. Whether particles can be pushed by the solid-liquid interface seems to depend on the particular system under consideration and it is not possible to be definitive about such an effect at this stage.

Whatever the mechanism leading to the nonuniform distribution of inclusions, it is evident that if austenite is the first phase to solidify, then numerous relatively large inclusions will be found at the austenite grain boundaries. This should have a very detrimental effect on toughness when allotriomorphic ferrite then forms at the austenite grain boundaries. It is emphasized that solidification mode will be austenitic either when the chemical composition at the fusion boundary is thermodynamically suitable to induce the epitaxial growth of austenite, or when the cooling rate and undercooling is high enough to kinetically favor austenite growth relative to that of δ-ferrite. The latter circumstance may arise with electron beam or laser beam welding and is to be investigated in future work.

V. CONCLUSIONS

For the welding conditions used in the present work, the deposition of a low-carbon electrode on a high-carbon substrate causes the weld pool to solidify as austenite, whereas solidification proceeds with δ-ferrite as the primary phase when a medium carbon electrode is deposited on a low-carbon substrate. This follows from the fact that weld pool solidification occurs by the epitaxial growth of grains at the fusion boundary, and it is the crystallographic structure of these which determines the solidification mode.

It is found that inclusions in low-alloy steel welds deposited by a manual-metal-arc technique are not uniformly distributed; they tend to locate themselves preferentially at the boundaries of the first phase to solidify. For an austenitic solidification mode, the inclusions are mostly located at the austenite grain boundaries and hence are present in the allotriomorphic ferrite which forms from the austenite at the grain boundaries. For solidification as δ-ferrite, the subsequent transformation to austenite ensures that most of the inclusions in the final weld are located away from the austenite grain boundaries, in regions where they can contribute toward the intragranular nucleation of acicular ferrite. This behavior dictates that welds which solidify as austenite (either because of a high-carbon substrate or because the welding process leads to a high cooling rate during solidification) should have relatively poor toughness.

The reason for the observed nonuniform distribution of inclusions can be attributed tentatively to surface tension effects at the solidification front (Marangoni effect) or to the pushing of inclusions by the solid-liquid interface.

REFERENCES

1. R. J. Pargeter and D. J. Abson: Proc. Conf., Welding Institute, Abington, U.K., 1982, paper 42, pp. 1-12.
2. T. Edvardsson, H. Fredriksson, and I. Svensson: Met. Sci., 1976, vol. 10, pp. 298-306.
3. H. K. D. H. Bhadeshia, L-E. Svensson, and B. Gretoft: Acta Metall., 1985, vol. 33, pp. 1271-83.
4. D. Widgery: Welding Institute Research Report, Welding Institute, Abington, U.K., Feb. 1973, M76/73.
5. J. H. Tweed: University of Cambridge, U.K., Ph.D. Thesis, 1982.
6. Y. Ito, M. Nakanishi, and Y. Komizo: Met. Constr., 1982, vol. 14, pp. 472-78.
7. Y. Ito, M. Nakanishi, and Y. Komizo: Sumitomo Search, 1979, vol. 21, pp. 52-67.
8. D. J. Widgery: Weld. J., 1976, vol. 55, Res. Supp., pp. 57s-68s.
9. J. H. Tweed and J. F. Knott: Met. Sci., 1983, vol. 17, pp. 45-54.
10. M. A. Munnig Schmidt-Van Der Burg, S. Hoekstra, and G. Den Outen: Weld. J., 1985, vol. 64, Res. Supp., pp. 63s-70s.
11. D. E. McRobie: University of Cambridge, U.K., Ph.D. Thesis, 1985.
12. J. F. Knott: Proc. Conf., Pergamon Press, Oxford, U.K., 1985, pp. 83-103.
13. Y. Ito and M. Nakanishi: Sumitomo Search, 1976, vol. 15, pp. 42-62.
14. D. J. Abson, R. E. Dolby, and P. H. M. Hart: Proc. Conf., Welding Institute, Abington, U.K., 1979, pp. 75-101.
15. S. Liu, C. B. Dallam, and D. L. Olson: Proc. Conf., Oak Ridge National Laboratory, Oak Ridge, TN 37830, 1982, pp. 445-65.
16. D. R. Uhlmann, B. Chalmers, and K. A. Jackson: J. Appl. Phys., 1964, vol. 35, pp. 2986-93.
17. G. F. Bolling and J. Cissé: J. Cryst. Growth, 1971, vol. 10, pp. 56-66.
18. J. Cissé and G. F. Bolling: J. Cryst. Growth, 1971, vol. 10, pp. 67-76.
19. A. A. Chernov, D. E. Temkin, and A. M. Mel'nikova: Kristall., 1976, vol. 21, pp. 652-60.

20. M. Dadian: *Proc. Conf.*, ASM, Metals Park, OH 44073, 1986, pp. 101-17.
21. B. Gretoft, H. D. K. H. Bhadeshia, and L-E. Svensson: *Acta Stereol.*, 1986, vol. 5, pp. 365-71.
22. Ö. Hammar and U. Svensson: *Proc. Conf.*, Metals Society, London, U.K., 1977, pp. 401-10.
23. I. Craig, T. H. North, and H. B. Bell: *Proc. Conf.*, Welding Institute, Abington, U.K., 1979, pp. 249-63.
24. E. T. Turkdogan: *J. Iron Steel Inst.*, 1966, vol. 204, pp. 914-19.
25. O. Grong, T. A. Siewert, G. P. Martins, and D. L. Olson: *Metall. Trans. A*, 1986, vol. 17A, pp. 1797-1807.
26. R. A. Woods and D. C. Milner: *Weld. J.*, 1971, vol. 50, Res. Supp., pp. 164s-171s.
27. K. E. Easterling: *Mat. Sci. Eng.*, 1984, vol. 64, pp. 191-98.
28. K. E. Easterling: *Introduction to the Physical Metallurgy of Welding*, 1st ed., Butterworth's & Co. Ltd., London, U.K., 1983, p. 63.
29. M. J. Tinkler, I. Grant, G. Mizumo, and C. Gluck: *Proc. Conf.*, Welding Institute, Abington, U.K., 1984, paper 29, pp. 1-13.
30. F. Weinberg: *Proc. Conf.*, National Aeronautics and Space Administration, Washington, DC 20546, 1984, pp. 79-90.
31. C. E. Schvezov and F. Weinberg: *Metall. Trans. B*, 1985, vol. 16B, pp. 367-75.